Supplement of Atmos. Chem. Phys., 23, 13049–13060, 2023
https://doi.org/10.5194/acp-23-13049-2023-supplement

Atmospheric Chemistry and Physics
Open Access

Supplement of

High enrichment of heavy metals in fine particulate matter through dust aerosol generation

Qianqian Gao et al.

Correspondence to: Hongliang Zhang (zhanghl@fudan.edu.cn), Jianmin Chen (jmchen@fudan.edu.cn), and Xiaofei Wang (xiaofeiwang@fudan.edu.cn)

Supplementary Information

This file includes 3 Texts, 8 Tables and 17 Figures:

Text S1. Soil texture characterization.

Text S2. Inverse Distance Weight (IDW).

Text S3. A one-way Analysis of Variance (ANOVA) analysis.

Table S1. The weight percent of heavy metal in dust-$PM_{2.5}$, dust-PM_{10} and dust-PM_{30} are shown in SPECIATE datasets.

Table S2. Soil properties: pH and soil texture.

Table S3. Mass collected in dust aerosols of $PM_{2.5}$ and PM_{10}.

Table S4. Mass collected in MOUDI samples.

Supplementary Figure S1. Soil sampling locations.

Supplementary Figure S2. Experimental setup.

Supplementary Figure S3. Comparison of the absolute concentrations of heavy metals in the S1-S14 natural soil samples and dust aerosols.

Supplementary Figure S4. Comparison of the absolute concentrations of heavy metals between natural soil samples and dust aerosols.

Supplementary Figure S5. Correlation between soils and PM_{10}.

Supplementary Figure S6. Significance between soils and $PM_{2.5}$ in heavy metals.

Supplementary Figure S7. The enrichment factor of heavy metals in $PM_{2.5}$ and PM_{10} dust aerosols.

Supplementary Figure S8. Particle size distribution of dust aerosols produced from S9 and S14.

Supplementary Figure S9. SEM images of the soil and dust aerosols (generated from S10).

Supplementary Figure S10. Absolute concentrations of heavy metals in MOUDI samples.

Supplementary Figure S11. Modeling of the contributions of As in dust aerosols to atmospheric heavy metals.

Supplementary Figure S12. Modeling of the contributions of Cu in dust aerosols to atmospheric heavy metals.

Supplementary Figure S13. Modeling of the contributions of Mn in dust aerosols to atmospheric heavy metal.

Supplementary Figure S14. Modeling of the contributions of Ti in dust aerosols to atmospheric heavy metals.

Supplementary Figure S15. Modeling of the contributions of Zn in dust aerosols to atmospheric heavy metal.

Supplementary Figure S16. Backward trajectories.

Supplementary Figure S17. Averaged mass spectra of dust particle cluster.

Text S1. Soil texture characterization

To measure the particle size distribution of the soil, approximately 0.03 to 0.5 g of air-dried soil samples were first passed through a 2 mm sieve. Subsequently, 10 mL of distilled water was added to the soil, and a dispersant was used to adjust the pH based on the soil's alkalinity or acidity. The dispersant consisted of either 1 to 1.5 mL of 0.5 mol/L hexametaphosphate (HMP) or 0.5 mol/L sodium hydroxide (NaOH). The mixture was then left to soak overnight before undergoing ultrasonic vibration for 2 minutes. Finally, the Laser Scattering Particle Size Distribution Analyzer (LA-960) was utilized to measure the soil samples labeled as S1-S14.

Text S2. Inverse Distance Weight (IDW)

IDW is a point-based interpolation method (Harman et al., 2016). The value at point (N_0) is calculated through the following formula.

$$N_0 = \frac{\sum_{i=1}^{n} N_i \cdot P_i}{\sum_{i=1}^{n} P_{ii}} \qquad (1)$$

Where n represents the number of measurement points. N_i represents the value at point i. P_i is the weight of the value at i position. The weight P_i can be calculated with Eq. (2) below as a function of the distance between the reference point and the interpolation point following from the idea that the effect of the closer points is higher than distance ones (Macedonio and Pareschi, 1991).

$$p_i = \frac{1}{d_i^k} \qquad i = 1, 2, \dots n \qquad (2)$$

Where d_i is the horizontal distance between the interpolation point at (x_0, y_0) and the reference points at (x_i, y_i) and is calculated by Eq. (3). k is the power of the distance.

$$d_i = \sqrt{(x_i - x_0)^2 + (y_i - y_0)^2} \qquad (3)$$

Text S3. A one-way Analysis of Variance (ANOVA) analysis

To examine the relationship between soil texture and their corresponding enrichment factors (EFs), a one-way Analysis of Variance (ANOVA) test was conducted using SPSS. When comparing the differences among the six types of sandy soils (S2, S4, S7, S10, S11, and S12), enter the average EF values (dust-$PM_{2.5}$ and dust-PM_{10}) for the six types of sandy soils in the software, and then select one-way ANOVA with a confidence level of 0.05.

To compare the differences in enrichment factors among different soil types, considering that the number of soil samples for each type was not equal, calculate the average enrichment factor for each type using two or more soil samples of the same type. Then, input the average enrichment factors (dust-$PM_{2.5}$ and dust-PM_{10}) for each type of soil (silty loam, sand, sandy loam, loam, loam sand, and silty clay loam) into the software and perform the aforementioned operations. The data and specific results can be found in Table S5-S8.

Table S1. The weight percent of heavy metal in dust-$PM_{2.5}$, dust-PM_{10} and dust-PM_{30} are shown in SPECIATE datasets (Profile NO.41350). Here, profile numbers 453102.5, 4531010 and 4531030 were used.

	Weight percent		
Heavy metal	$PM_{2.5}$	PM_{10}	PM_{30}
V	0.014	0.015	0.012
Cr	0.011	0.013	0.013
Mn	0.096	0.103	0.056
Ni	0.004	0.004	0.008
Cu	0.035	0.05	0.044
Zn	0.039	0.045	0.042
As	0	0.002	0.002
Cd	0.008	0.004	0.003
Ba	0	0.012	0.042
Ti	0.335	0.362	0.171
Pb	0.053	0.044	0.05

Table S2. Soil properties: pH and soil texture

Soil Number	Location	pH	Soil texture
S1	Ulanqab, Inner Mongolia	7.8	silty loam
S2	Bai Yin Chagan, Inner Mongolia	7.5	sand
S3	Bai Yin Chagan, Inner Mongolia	7.7	sandy loam
S4	Hohhot, Inner Mongolia	7.7	sand
S5	Yumen East Town, Jiayuguan	8.1	loam
S6	Yinda Town, Jiayuguan	8.0	loam
S7	Xitushan, Jiayuguan	8.0	sand
S8	Yema Bay, Jiayuguan	7.7	loamy sand
S9	Pingliang City, Gansu Province	7.6	silty clay loam
S10	Alxa, Inner Mongolia	8.1	sand
S11	Alxa, Inner Mongolia	8.1	sand
S12	Alxa, Inner Mongolia	7.9	sand
S13	Bayingoleng, Xinjiang	7.9	loamy sand
S14	Fudan university, Shanghai	7.5	silty clay loam

Table S3. Mass collected in dust aerosols of $PM_{2.5}$ and PM_{10}.

EXP	S1 mass (g)	S2 mass (g)	S3 mass (g)	S4 mass (g)	S5 mass (g)	S6 mass (g)	S7 mass (g)	S8 mass (g)	S9 mass (g)	S10 mass (g)	S11 mass (g)	S12 mass (g)	S13 mass (g)	S14 mass (g)
$PM_{2.5}$-1	0.0034	0.0498	0.0271	0.0186	0.0322	0.015	0.013	0.0261	0.0257	0.0229	0.012	0.0343	0.0534	0.0751
$PM_{2.5}$-2	0.044	0.0424	0.0309	0.0228	0.0293	0.0221	0.0198	0.0341	0.0171	0.0297	0.0199	0.0388	0.0529	0.0585
$PM_{2.5}$-3	0.0368	0.021	0.0244	0.0245	0.0181	0.0149	0.0219	0.0335	0.0321	0.0375	0.0232	0.0337	0.0564	0.0859
PM_{10}-1	0.0738	0.0706	0.0521	0.0543	0.0606	0.0376	0.0591	0.081	0.0898	0.0806	0.097	0.0653	0.0903	0.0607
PM_{10}-2	0.0743	0.0765	0.0877	0.0384	0.0579	0.0255	0.0505	0.0732	0.0849	0.0749	0.126	0.0602	0.0872	0.0769
PM_{10}-3	0.0775	0.0691	0.0765	0.0282	0.0625	0.0266	0.0592	0.0765	0.089	0.0845	0.0772	0.0674	0.0922	0.0763

Table S4. Mass collected in MOUDI samples. Here, an S10 sample was used.

Sample	EXP1	EXP2	EXP3
	mass (g)	mass (g)	mass (g)
PM >10	0.0738	0.0891	0.0476
PM 5.6~10	0.0315	0.0531	0.0112
PM 3.2~5.6	0.0243	0.0381	0.0132
PM 1.8~3.2	0.0176	0.0206	0.0074
PM 1.0~1.8	0.0059	0.0102	0.0074
PM 0.56~1.0	0.0056	0.0037	0.0032

Table S5. A one-way Analysis of Variance (ANOVA) analysis was conducted in dust-$PM_{2.5}$ among sandy soils (S2, S4, S7, S10, S11, and S12).

Origin of disparities	SS	df	MS	F	*P*-value	F crit
Between the group	15.62294	5	3.124589	3.79773	0.004393	2.353809
Within the group	54.30161	66	0.822752			
Total	69.92456	71				

Table S6. A one-way Analysis of Variance (ANOVA) analysis was conducted in dust-PM_{10} among sandy soils (S2, S4, S7, S10, S11, and S12).

Origin of disparities	SS	df	MS	F	*P*-value	F crit
Between the group	14.74211	5	2.948422	31.17927	3.79E-16	2.353809
Within the group	6.241193	66	0.094564			
Total	20.9833	71				

Table S7. A one-way Analysis of Variance (ANOVA) analysis was conducted in dust-$PM_{2.5}$ among six different soil types (silty loam; sand; sandy loam; loam; loam sand and silty clay loam).

Origin of disparities	SS	df	MS	F	*P*-value	F crit
Between the group	78.82538	5	15.76508	15.56416	4.28E-10	2.353809
Within the group	66.852	66	1.012909			
Total	145.6774	71				

Table S8. A one-way Analysis of Variance (ANOVA) analysis was conducted in dust-PM_{10} among six different soil types (silty loam; sand; sandy loam; loam; loam sand and silty clay loam).

Origin of disparities	SS	df	MS	F	*P*-value	F crit
Between the group	6.130101	5	1.22602	19.79507	5.35E-12	2.353809
Within the group	4.087752	66	0.061936			
Total	10.21785	71				

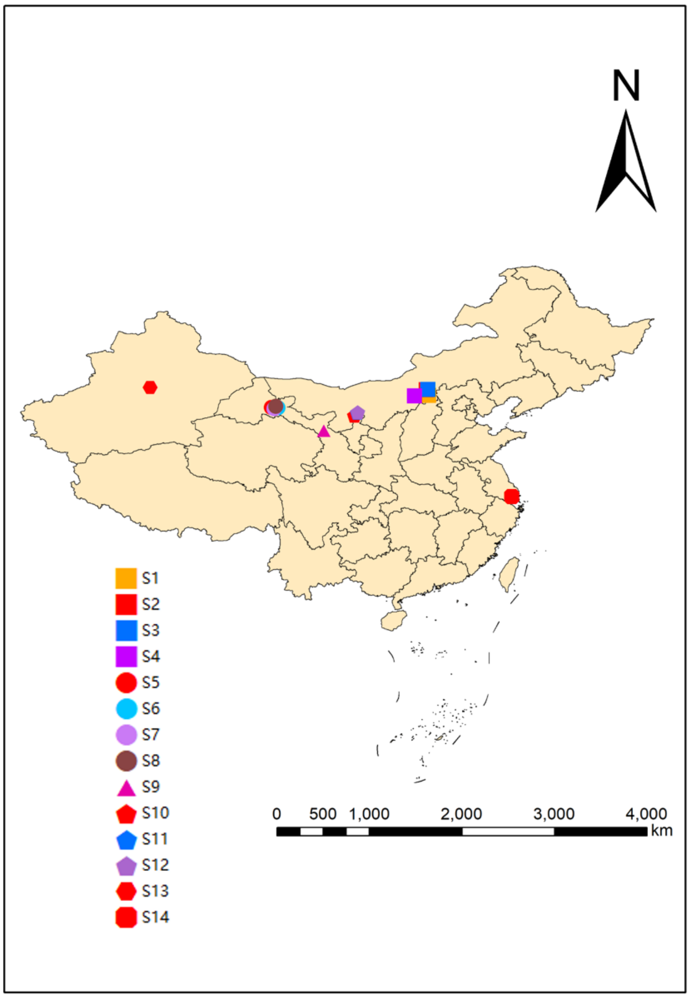

Supplementary Figure S1. Soil sampling locations. S1-S4 were collected from dust sources of the northern slope of Yin-shan Mountain in central inner Mongolia and the adjacent areas of the Hunshandake Sandy Land (S1: 113.26°E, 41.01°N; S2: 113.0°E, 41.55°N; S3: 113.13, 41.58°N; S4: 111.85°E, 40.93), S5-S12 were collected from dust sources of Hexi Corridor and Alxa Plateau (S5: 97.92°E, 39.81°N; S6: 98.56°E, 39.80°N; S7: 98.20°E, 39.7°N; S8: 98.37°E, 39.94°N; S9: 103.02°E, 37.59°N; S10: 106.01°E, 39.05°N; S11: 106.31°E, 39.34°N; S12: 106.33°E, 39.37°N); S13 was collected in Xinjiang Province, in the dust sources of the Taklimakan Desert (86.15°E, 41.76°N), and S14 was sampled from Shanghai Yangpu District (121.51°E, 31.34°N).

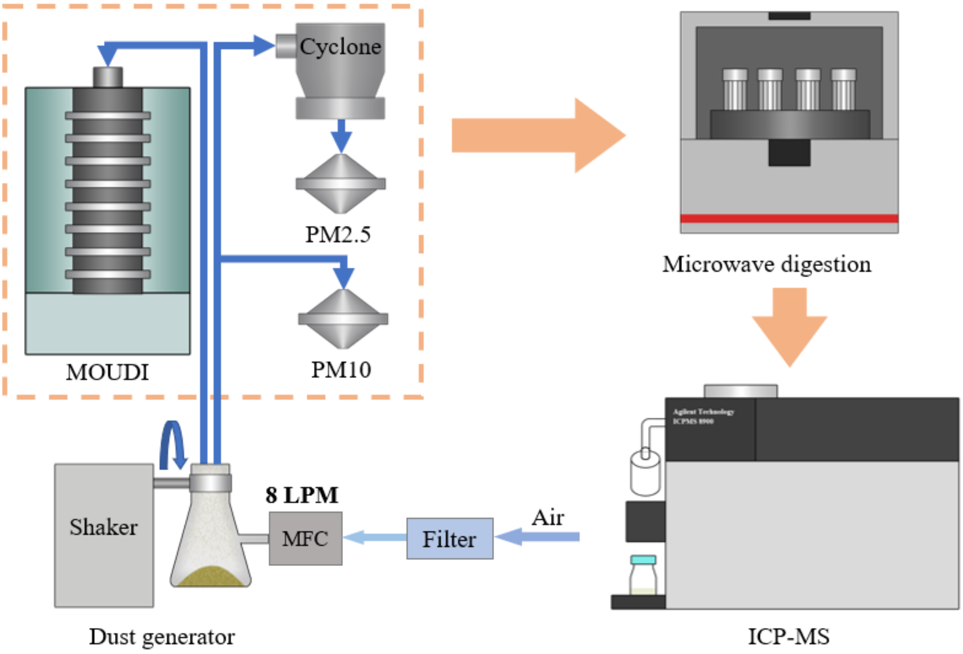

Supplementary Figure S2. Experimental setup. The setup consists of four parts: a dust generation system (Shaker), a dust particle size separation system ($PM_{2.5}$ Cyclone and MOUDI), a dust collection system (Filter holder), and the chemical analysis instrument (ICP-MS).

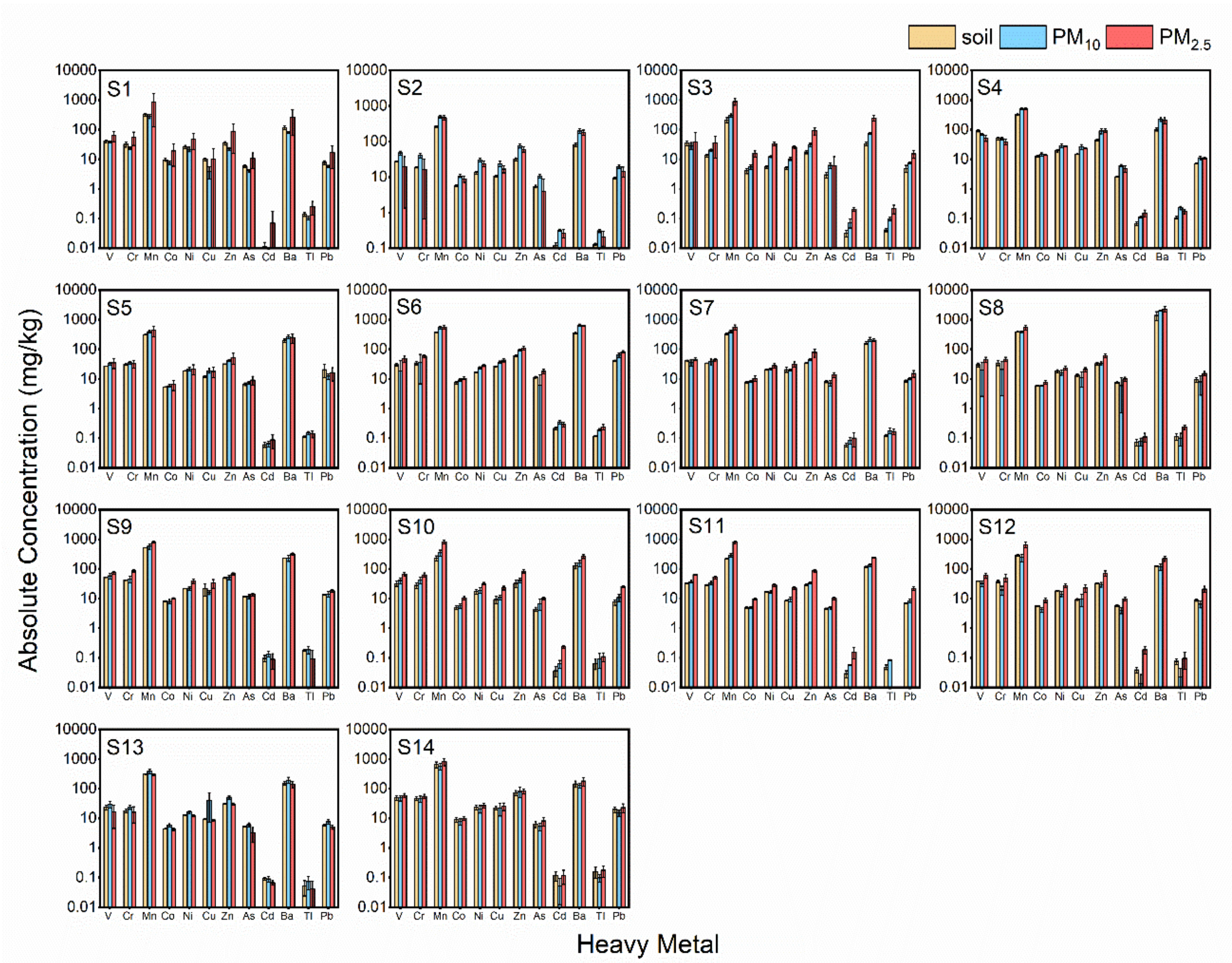

Supplementary Figure S3. Comparison of the absolute concentrations of heavy metals in the S1-S14 natural soil samples and dust aerosols. The whiskers on the bars represent the standard deviations of triplicates.

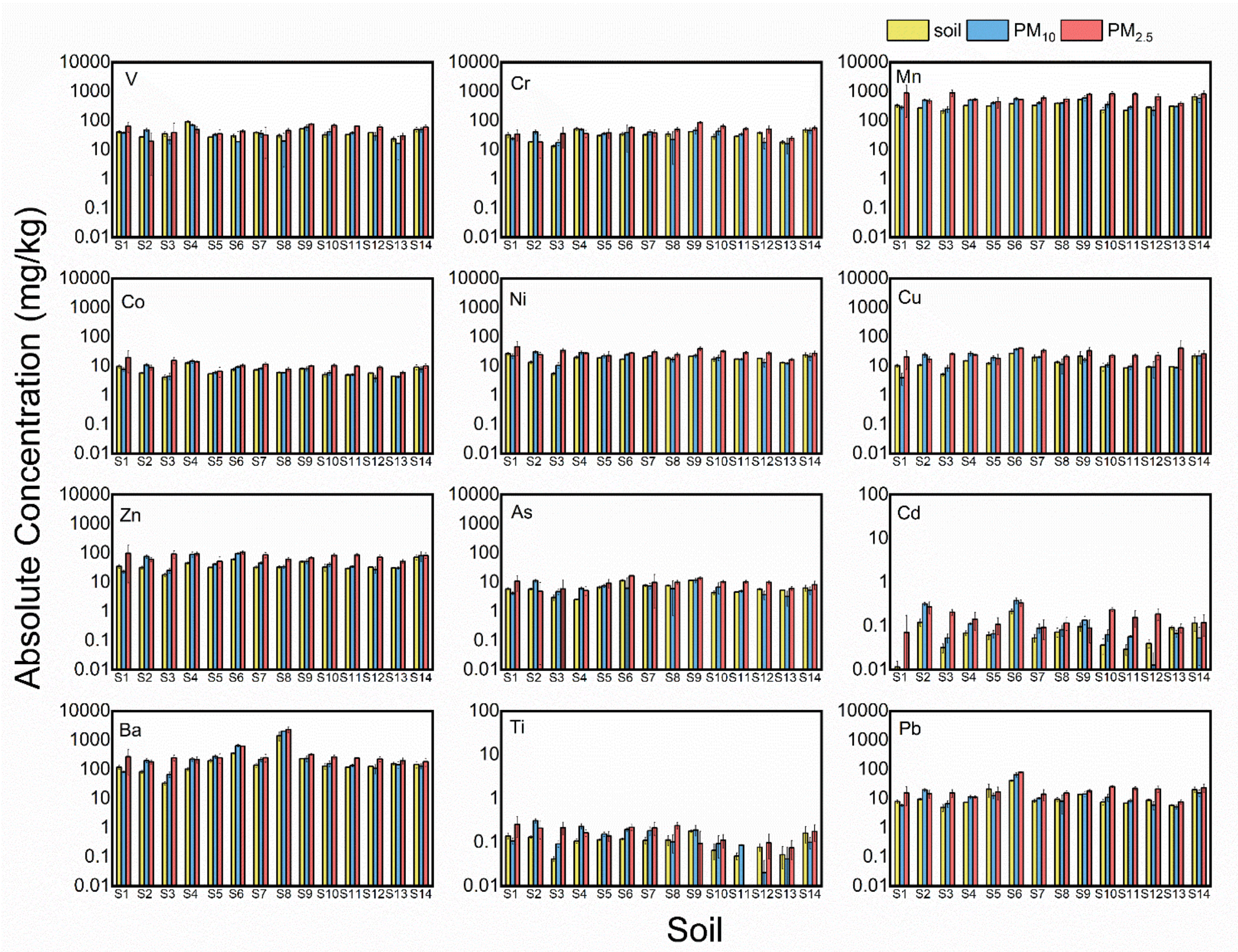

Supplementary Figure S4. Comparison of the absolute concentrations of heavy metals between natural soil samples and dust aerosols. The whiskers on the bars represent the standard deviations of triplicates.

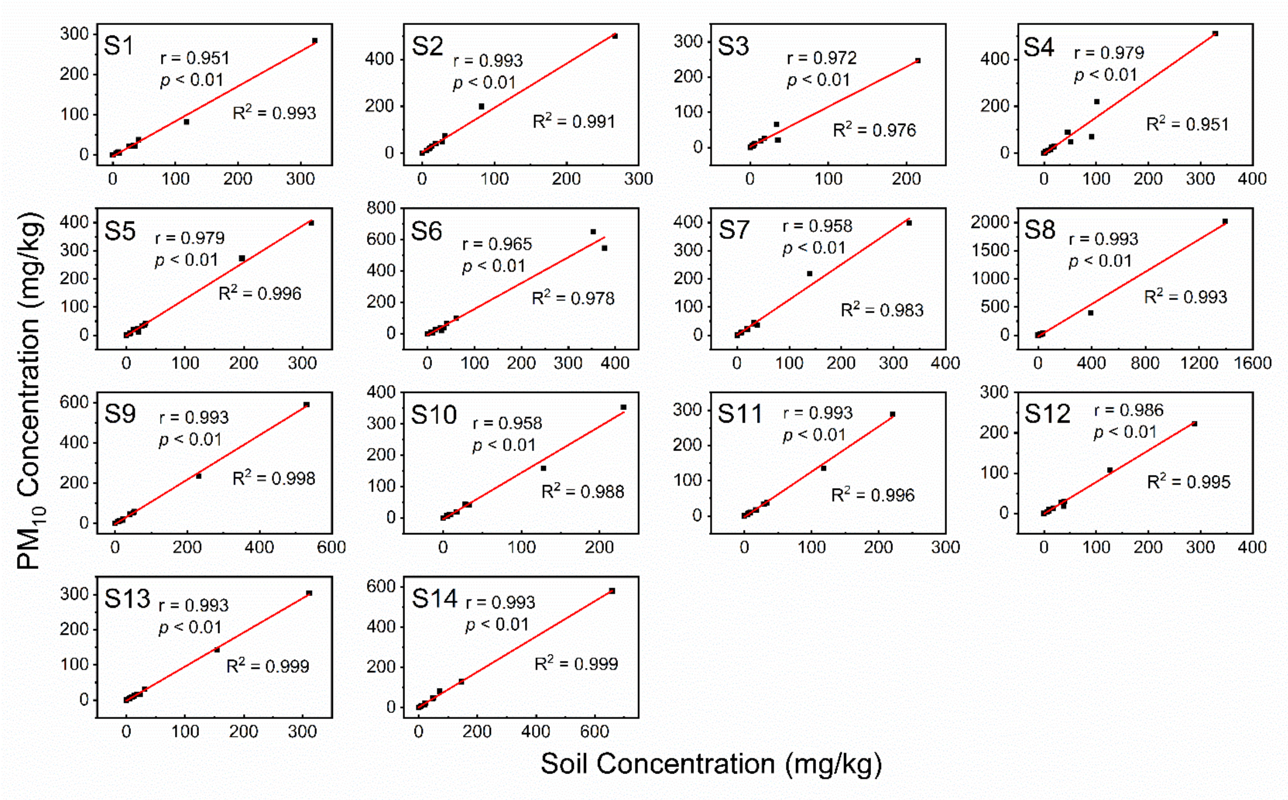

Supplementary Figure S5. Correlation between soils and PM_{10}. PM_{10} obtained by S1-S14 was compared with parent soils.

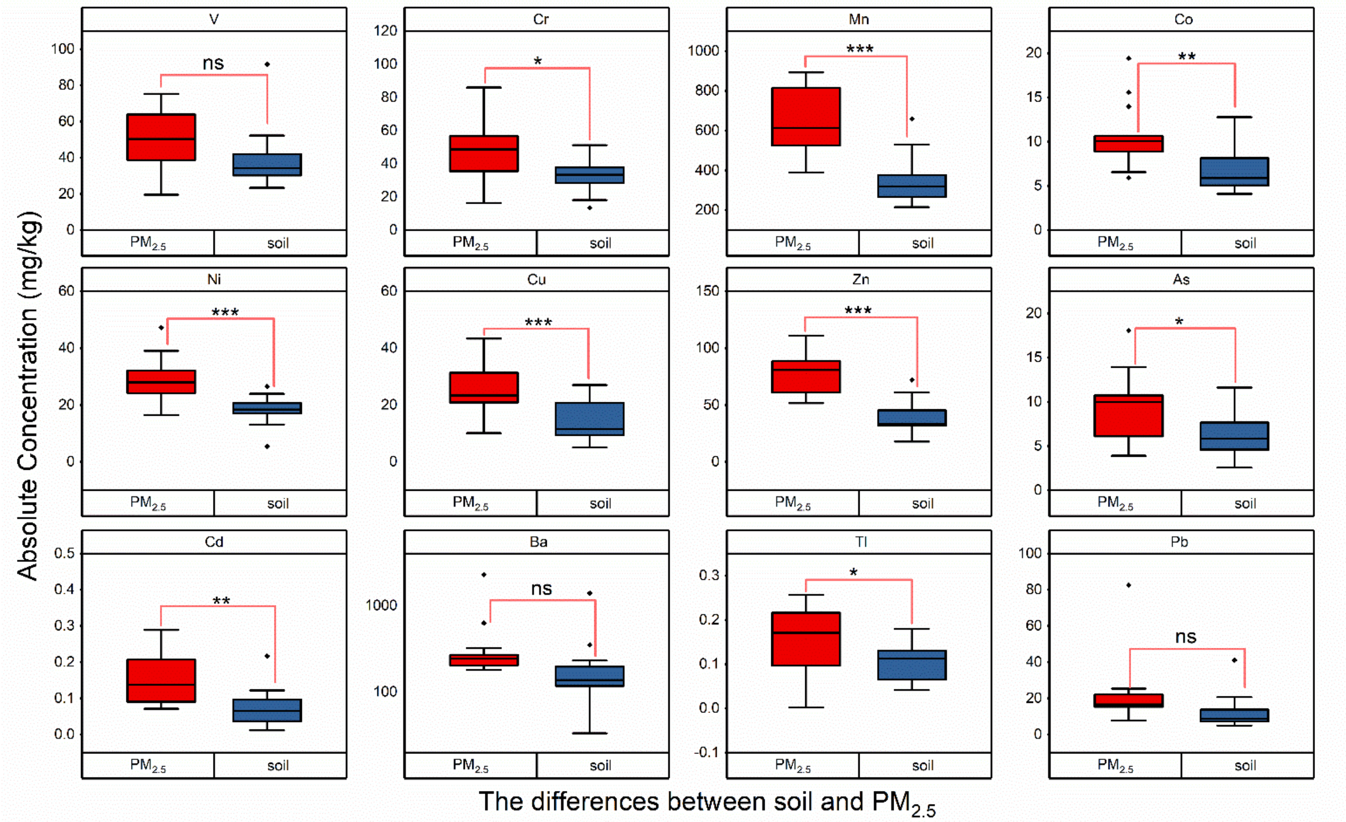

Notes: ns: not significant

∗: $0.05<p<0.01$

∗∗: $0.01<p<0.001$

∗∗∗: $p<0.001$

Supplementary Figure S6. Significance of the differences in heavy metal contents between soils and $PM_{2.5}$. Heavy metals in dust-$PM_{2.5}$ obtained by S1-S14 were compared with parent soils.

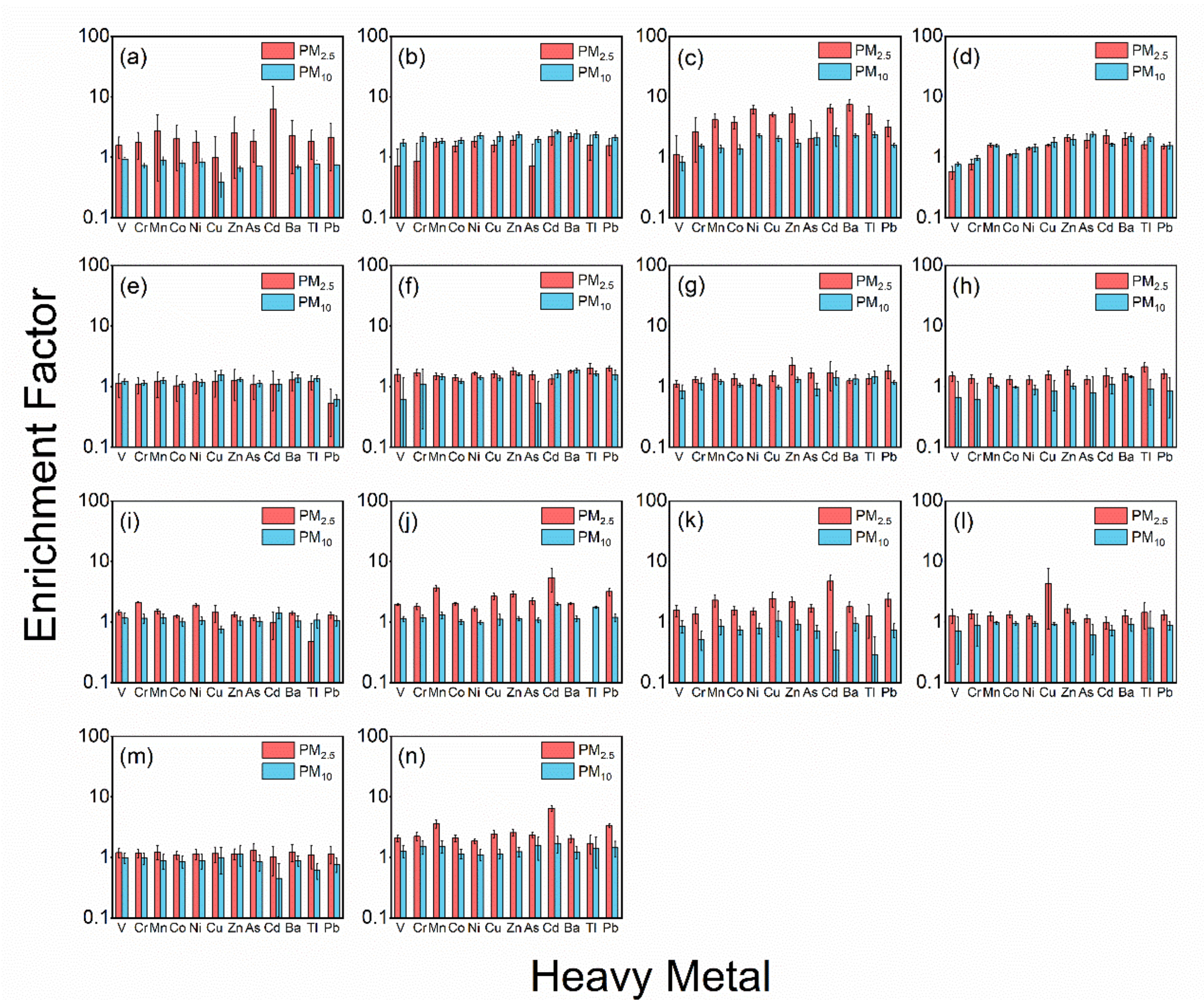

Supplementary Figure S7. Enrichment factor of heavy metals in dust-$PM_{2.5}$ and dust-PM_{10}.

The whiskers on the bars represent the standard deviations of triplicates.

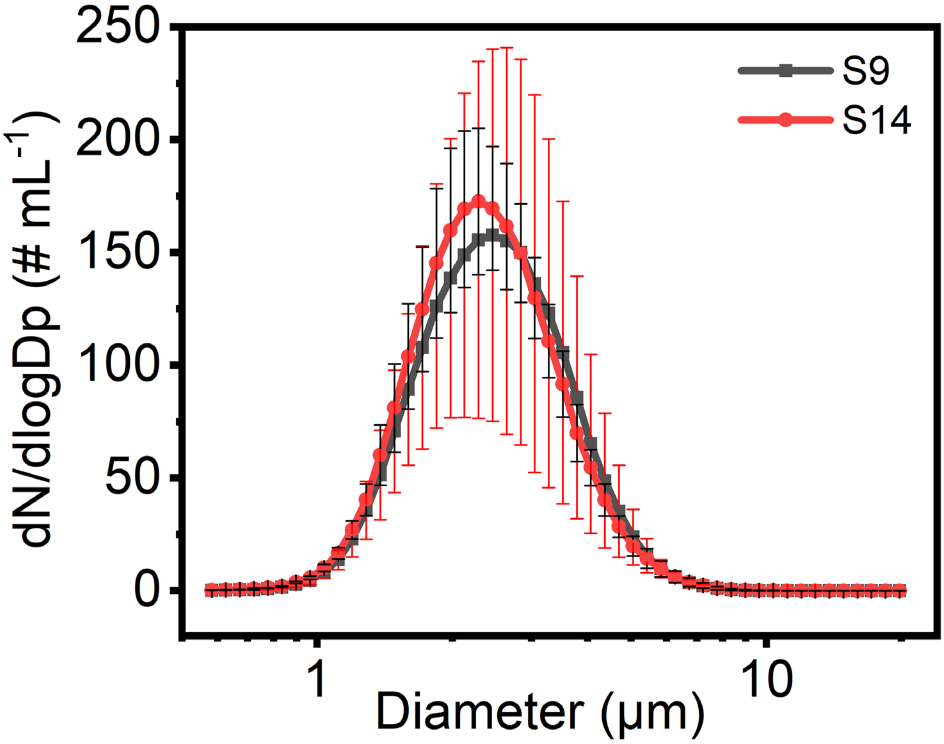

Supplementary Figure S8. Particle size distribution of dust aerosols produced from soil S9 and S14. The size distribution was detected by an Aerodynamic Particle Sizer (APS), which size range are 0.5-20 μm.

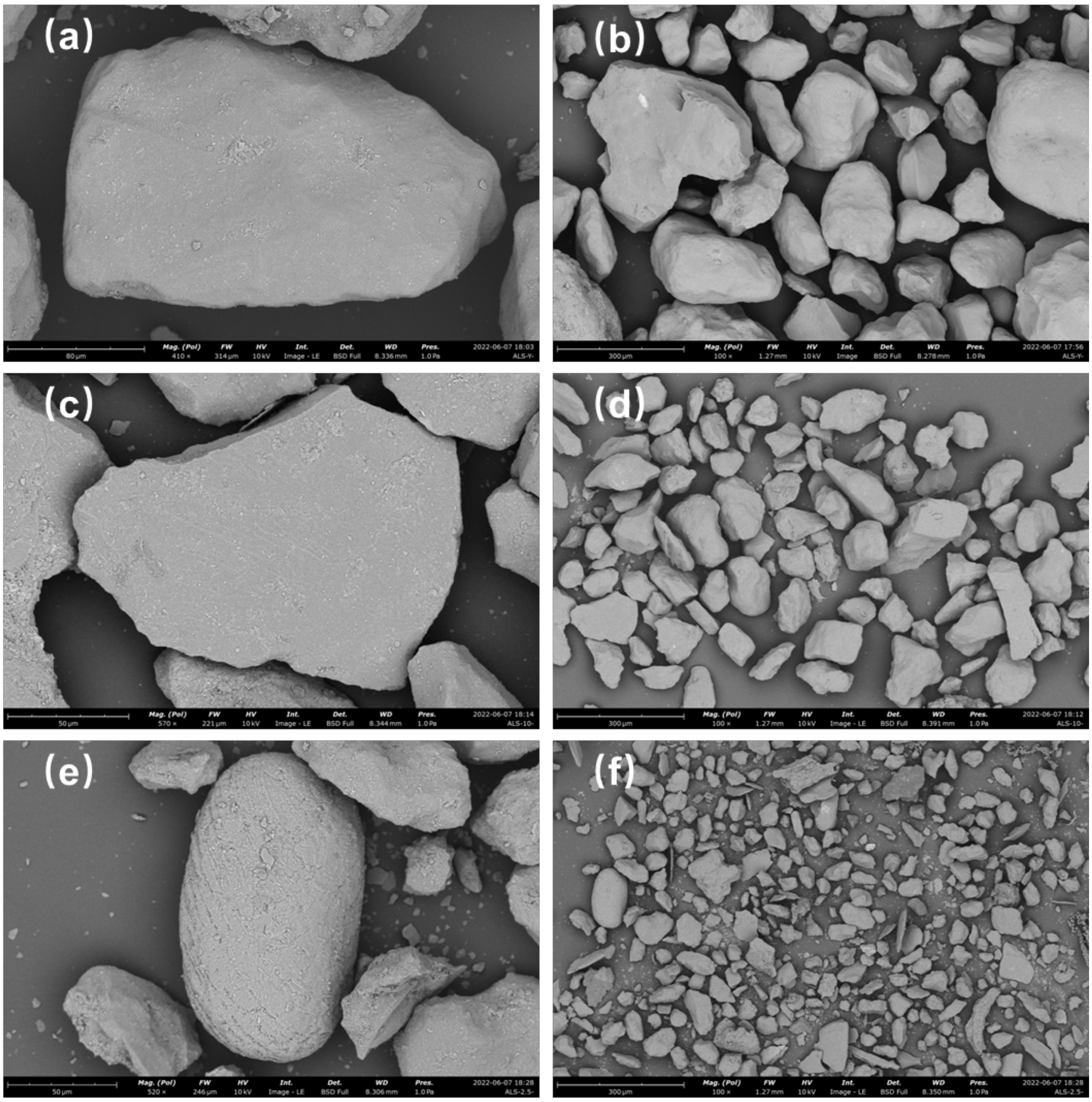

Supplementary Figure S9. SEM images of the soil and dust aerosols (generated from soil S10).

(a) and (b) are natural soil images; (c) and (d) are dust-PM_{10}; and (e), (f) are dust-$PM_{2.5}$.

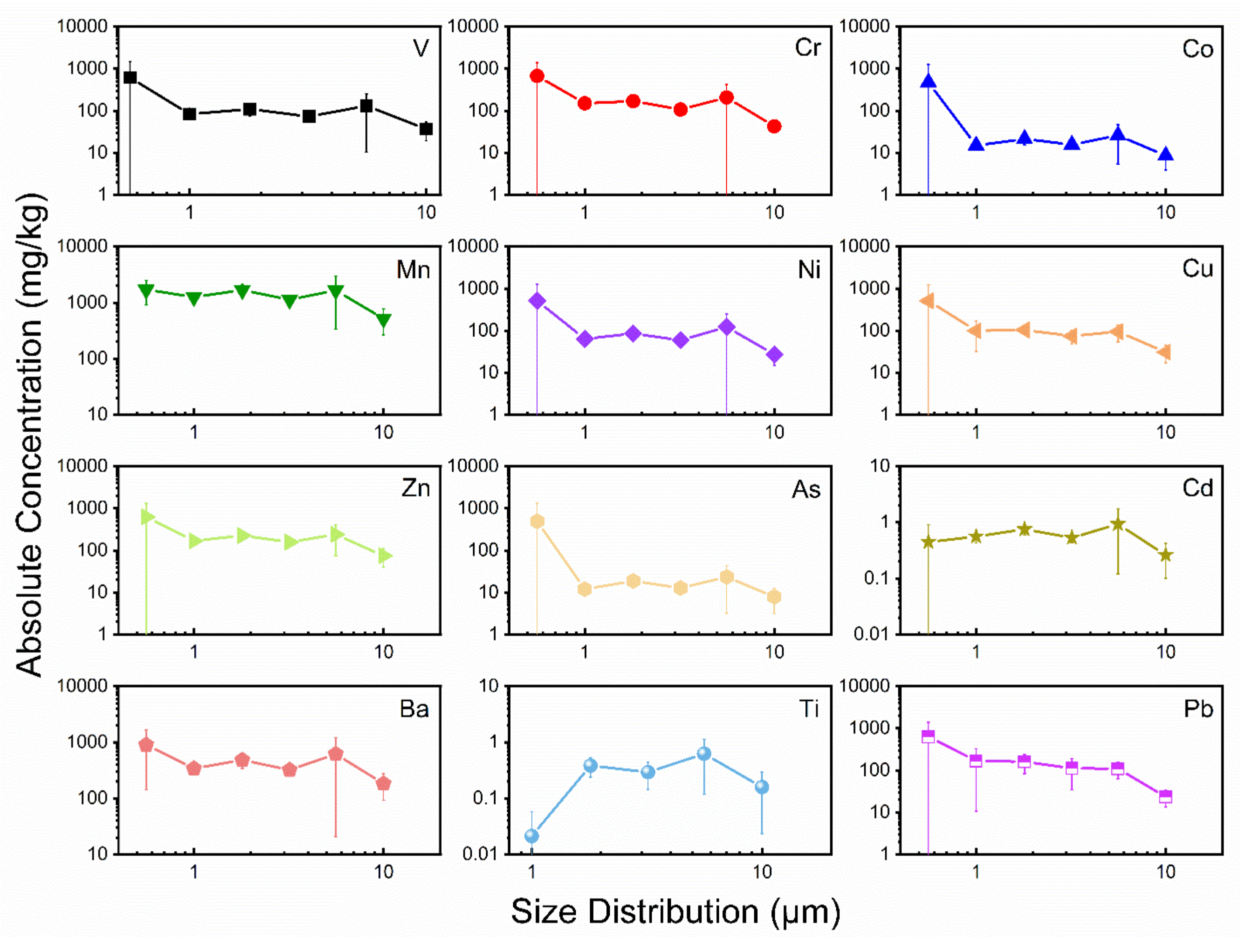

Supplementary Figure S10. Absolute concentrations of heavy metals in MOUDI samples. The particles sizes are above 10 μm, 5.6-10 μm, 3.2-5.6 μm, 1.8-3.2 μm, 1.0-1.8 μm, and 0.56-1.0 μm, respectively. Here, soil S10 was used.

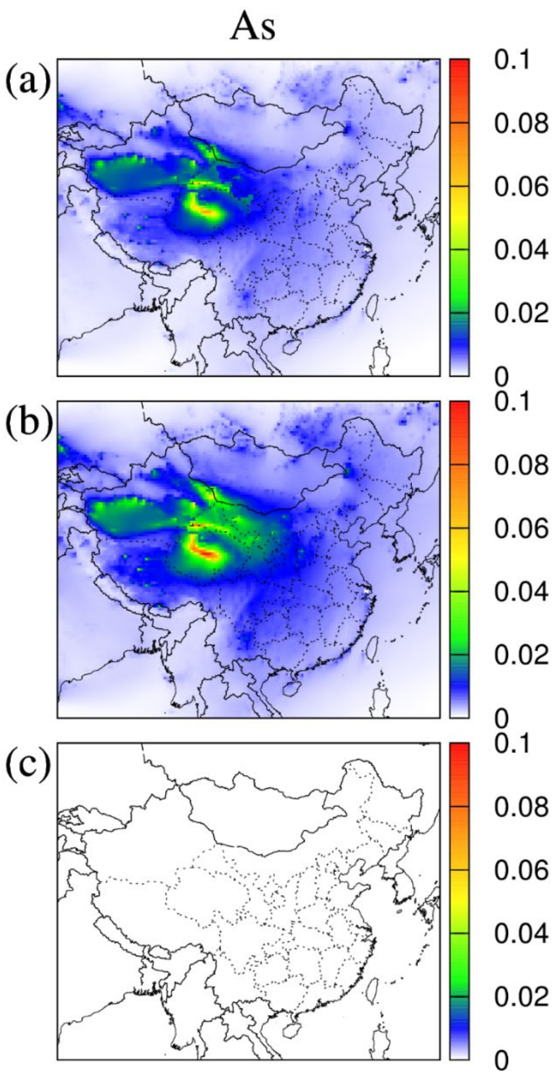

Supplementary Figure S11. Modeling of the contributions of As in dust aerosols to atmospheric heavy metals. These show the modeled results of As using the dust profiles of measured soil (a), dust-$PM_{2.5}$ (b), and the SPECIATE datasets (c). The unit is $\mu g/m^3$.

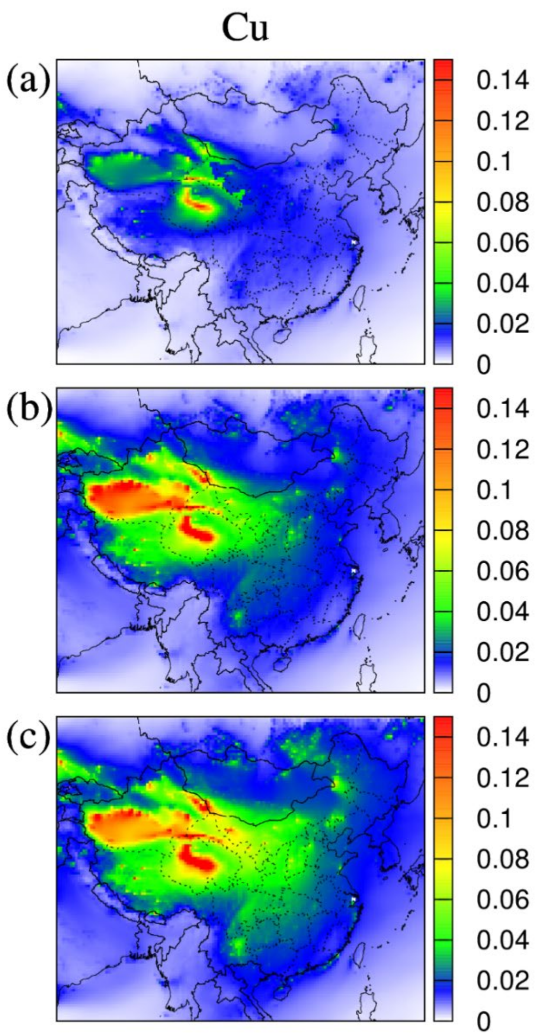

Supplementary Figure S12. Modeling of the contributions of Cu in dust aerosols to atmospheric heavy metals. These show the modeled results of Cu using the dust profiles of measured soil (a), dust-$PM_{2.5}$ (b), and the SPECIATE datasets (c). The unit is $\mu g/m^3$.

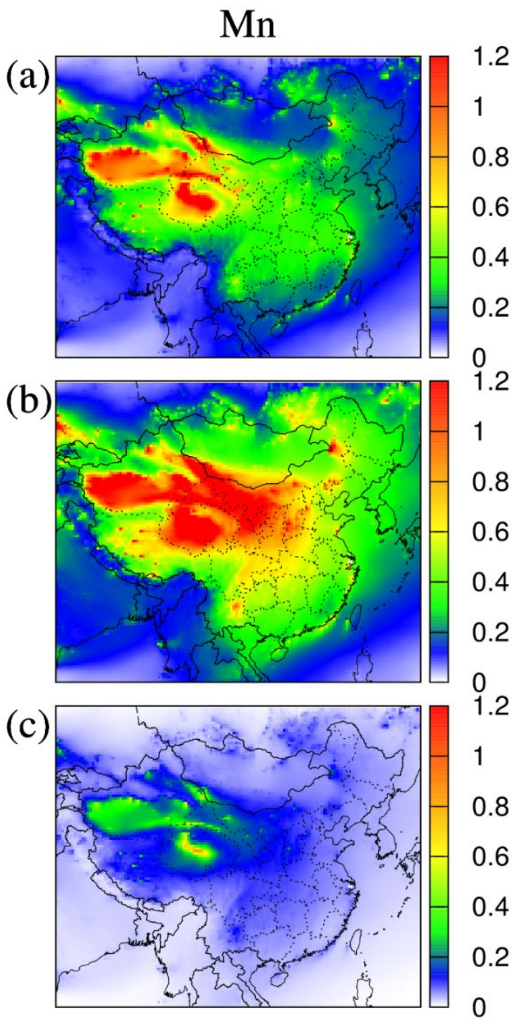

Supplementary Figure S13. Modeling of the contributions of Mn in dust aerosols to atmospheric heavy metals. These show the modeled results of Mn using the dust profiles of measured soil (a), dust-$PM_{2.5}$ (b), and the SPECIATE datasets (c). The unit is $\mu g/m^3$.

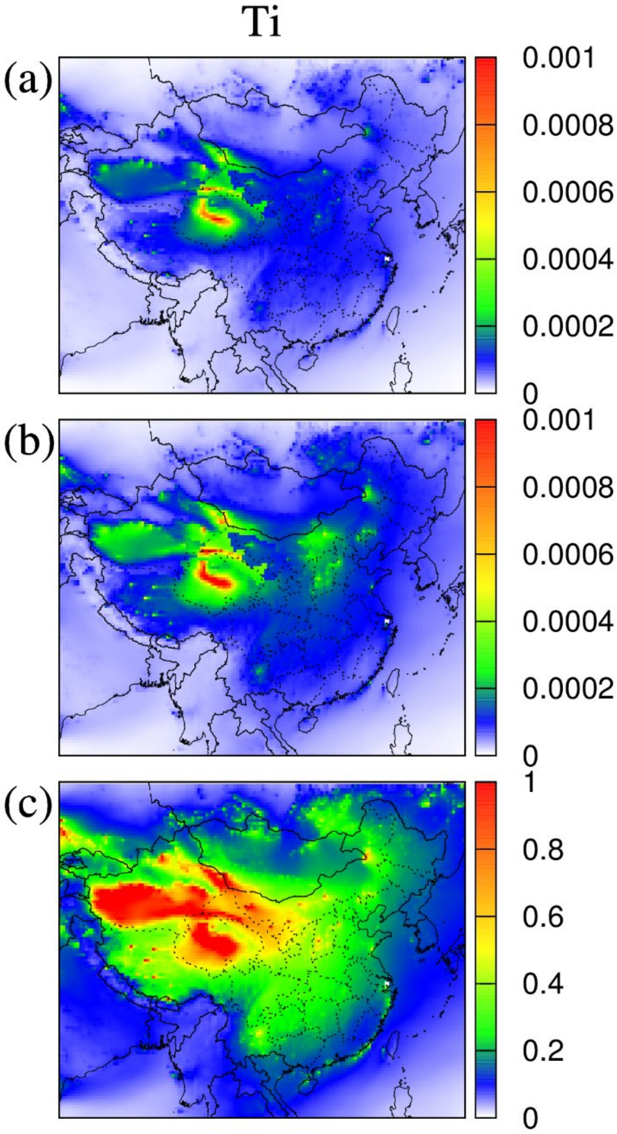

Supplementary Figure S14. Modeling of the contributions of Ti in dust aerosols to atmospheric heavy metals. These show the modeled results of Ti using the dust profiles of measured soil (a), dust-$PM_{2.5}$ (b), and the SPECIATE datasets (c). The unit is $\mu g/m^3$.

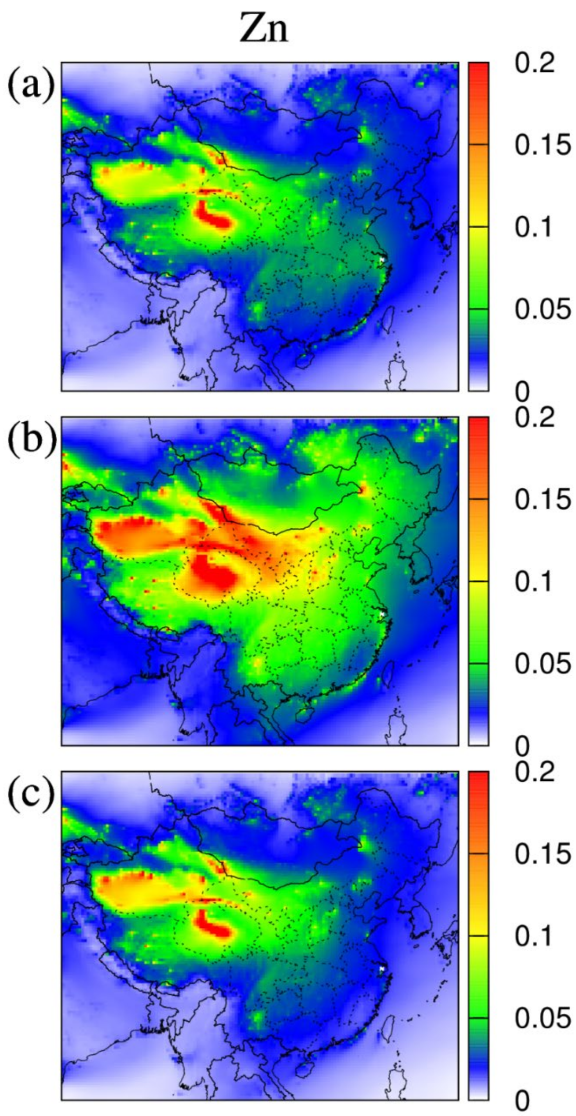

Supplementary Figure S15. Modeling of the contributions of Zn in dust aerosols to atmospheric heavy metals. These show the modeled results of Zn using the dust profiles of measured soil (a), dust-$PM_{2.5}$ (b), and the SPECIATE datasets (c). The unit is $\mu g/m^3$.

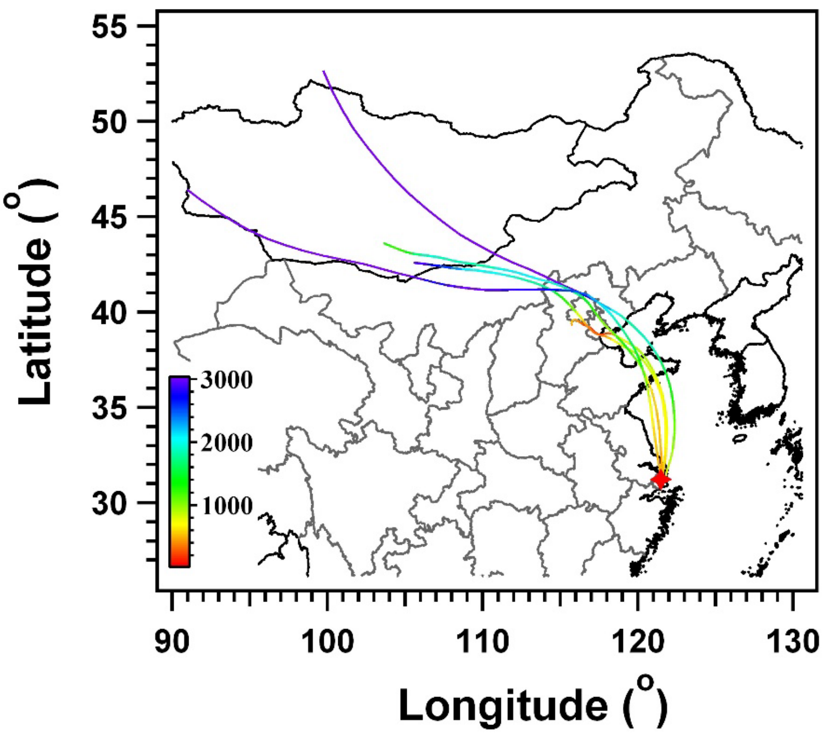

Supplementary Figure S16. Backward trajectories. The HYSPLIT 48-hour air mass backward trajectories at 500 m arrival height ending at 22:00 UTC+8 on 23 May, 2018.

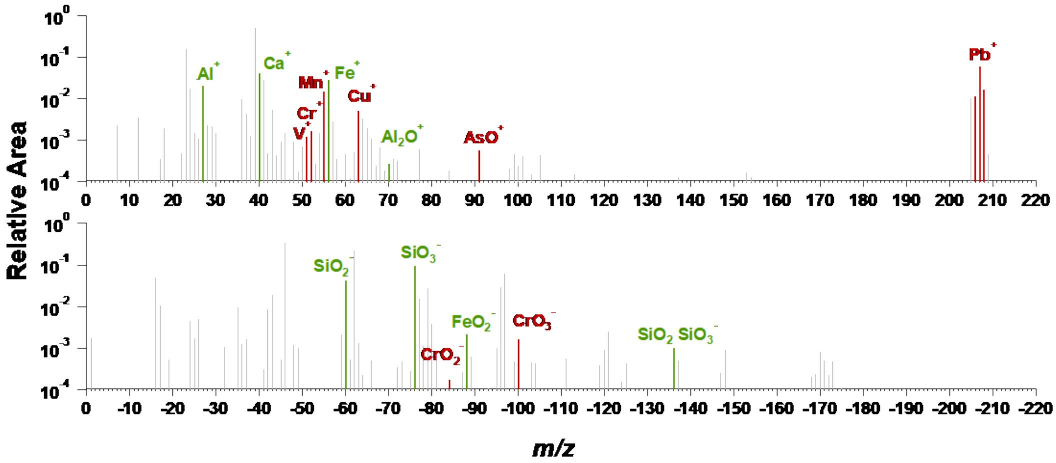

Supplementary Figure S17. Averaged mass spectra of dust particle cluster. The green sticks are typical dust markers; the red sticks are typical heavy metal markers.

Reference

Harman, B. I., Koseoglu, H., and Yigit, C. O.: Performance evaluation of IDW, Kriging and multiquadric interpolation methods in producing noise mapping: A case study at the city of Isparta, Turkey, Applied Acoustics, 112, 147-157, 10.1016/j.apacoust.2016.05.024, 2016.

Macedonio, G. and Pareschi, M. T.: An algorithm for the triangulation of arbitrarily distributed points - Applications to volume estimate and terrain fitting Computers & Geosciences, 17, 859-874, 10.1016/0098-3004(91)90086-s, 1991.